Talanta Open 5 (2022) 100091

Contents lists available at ScienceDirect

Talanta Open

journal homepage: www.sciencedirect.com/journal/talanta-open

Parallel plate wet denuder coupled ammonia transfer device-conductivity detector for near-real-time monitoring of gaseous ammonia

Haruka Tanaka [a], Makoto Namikawa [a], Naoya Tomiyasu [a], Hideji Tanaka [a,b], Masaki Takeuchi [a,b,*]

[a] Faculty of Pharmaceutical Sciences, Tokushima University, 1-78-1 Shomachi, Tokushima 770-8505, Japan
[b] Graduate School of Biomedical Sciences, Tokushima University, 1-78-1 Shomachi, Tokushima 770-8505, Japan

ARTICLE INFO

Keywords:
Ammonia
Denuder
Ammonia transfer device
Conductivity detection
Flow analysis

ABSTRACT

Gaseous ammonia (NH_3) is a primary basic substance in the atmosphere, and its global emission has been increasing in recent decades. It is vital to continuously monitor the atmospheric NH_3 to clarify the impact of NH_3 on sensitive ecosystems. This paper proposes a simple gaseous NH_3 monitor utilizing a parallel plate wet denuder (PPWD) and a conductometric flow injection analysis (FIA) with an ammonia transfer device (ATD). In the present study, water-soluble basic gases, NH_3, are selectively detected by the conductivity detector (CD). The ATD-CD ammonium detector requires no coloring reagents commonly used in FIA. Five-day field measurement of ambient NH_3 was successfully performed with 30 min time resolution. All the air samples over the observation period (n = 186) contained NH_3 above the limit of quantification (11.4 nmol m^{-3}). The NH_3 data showed excellent agreement with the values using ion chromatography in the field measurements.

1. Introduction

Gaseous ammonia (NH_3) is the primary basic gas in the atmosphere [1]. The sources of NH_3 emissions include agriculturalactivities such as animal husbandry and fertilization [2,3] and emissions from traffic and industrial activities [4,5]. In the atmosphere, NH_3 plays a crucial component in atmospheric chemistry, e.g., neutralizing material for cloud pH and precipitation, a precursor for secondary particulate formation [1,6]. Particulate ammonium constitutes a significant fraction of $PM_{2.5}$ and causes a reduction of atmospheric visibility through light extinction [7]. Excessive deposition of ammonium salts on sensitive ecosystems leads to soil acidification and surface water eutrophication [8]. Long-term exposure to fine particulate matter contributes to respiratory, cardiovascular, and other diseases [9,10]. Global emission of NH_3 has been increasing in recent decades [11,12], and its impact on the environment and public health would be highly significant. It is, therefore, critical to monitor atmospheric NH_3 and clarify its behavior in the environment.

Several gaseous NH_3 measurement techniques have been reported. Filter-based samplers and reagent-coated diffusion denuders are inexpensive and straightforward methods to collect gaseous NH_3. However, they have disadvantages of being time-consuming to analyze and having a low temporal resolution of 12 or 24 h. Open-path differential optical absorption spectroscopy [13] and quantum cascade laser absorption spectroscopy [14] can provide a fast response and high time resolution data. An online gas collector coupled with an NH_3 detection system enables near-real-time monitoring of gaseous NH_3. Ion chromatography is useful for quantifying ammonium (NH_4^+) in environmental water samples. Fluorometric/spectrophotometric flow injection analysis (FIA) is a portable and inexpensive alternative approach but requires fluorescent/colorimetric reagents or indicators to detect NH_4^+ [15–18]. Recently, a conductometric determination of NH_4^+ separated by membrane-based diffusion or distillation has been reported [19–21]. Many fluorometric/spectrophotometric and electrochemical NH_4^+ detection methods, including the above approaches are summarized in recent review papers [22,23].

In the present study, a parallel plate wet denuder, PPWD [24–27], and a conductometric FIA system with an ammonia transfer device, ATD, were used as a continuous gas collector and an NH_4^+ detector, respectively. Commercial carbonate removal device, CRD developed by Ullah et al. [28], worked as the ATD. The proposed method requires no fluorescent/colorimetric reagents that specifically react with NH_4^+, and atmospheric NH_3 is selectively detected online via PPWD, cation concentrator, ATD, conductivity detector, CD. First, a series of

* Corresponding author at: Graduate School of Biomedical Sciences, Tokushima University, 1-78-1 Shomachi, Tokushima 770-8505, Japan.
E-mail address: masaki.takeuchi@tokushima-u.ac.jp (M. Takeuchi).

https://doi.org/10.1016/j.talo.2022.100091
Received 25 December 2021; Received in revised form 28 January 2022; Accepted 28 January 2022
Available online 29 January 2022
2666-8319/© 2022 The Authors. Published by Elsevier B.V. This is an open access article under the CC BY license (http://creativecommons.org/licenses/by/4.0/).

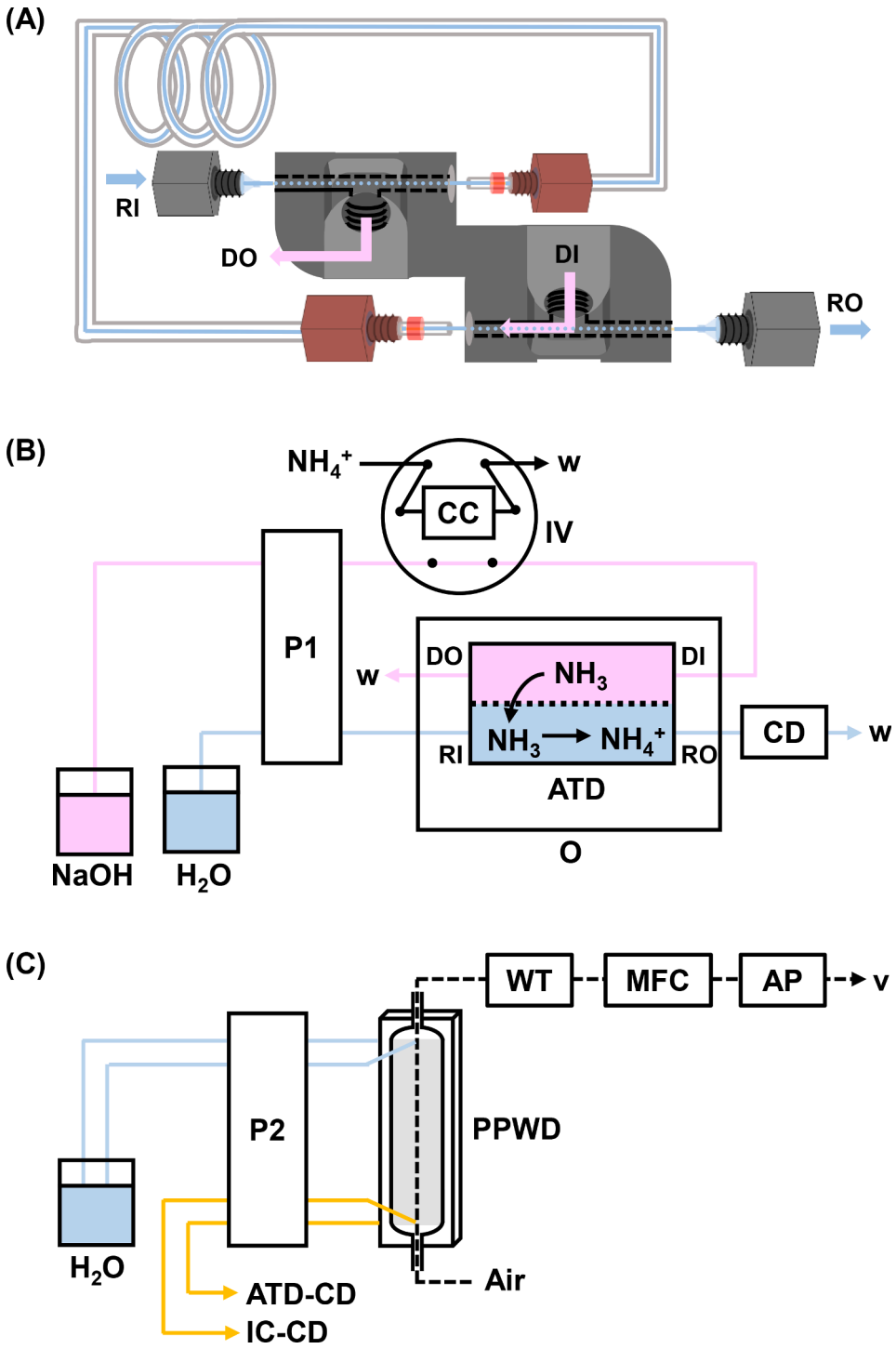

Fig. 1. Schematic of (A) ATD, (B) ATD-CD for NH_4^+ detection, (C) wet denuder coupled ATD-CD for atmospheric NH_3 monitoring. DI, donor inlet; DO, donor outlet; RI, receptor inlet; RO, receptor outlet; P1 & P2, peristaltic pump; IV, 6-port valve; CC, cation concentrator; O, oven; ATD, ammonia transfer device; CD, conductivity detector; *w*, waste; PPWD, parallel plate wet denuder; WT, water trap; MFC, mass flow controller; AP, air pump; IC, ion chromatograph; *v*, vent.

laboratory experiments have been conducted to optimize the ATD-CD, including elution time of NH_4^+ from concentrator, concentration and flow rate of donor solution, and ATD temperature. Then, optimized ATD-CD was compared with fluorometric/spectrophotometric FIA in the literature. Finally, the PPWD coupled ATD-CD was constructed as an online gaseous NH_3 monitor and evaluated in the field application.

2. Experimental

2.1. Reagents and ion chromatographic system

All reagents used in the present study (sodium hydroxide from Kanto Chemical, ammonium chloride from Katayama Chemical Industry, methanesulfonic acid from Kishida Chemical) were analytical grade and were used without further purification. Sartorius arium 611DI grade deionized water (> 18 MΩ cm) was used throughout. Cation

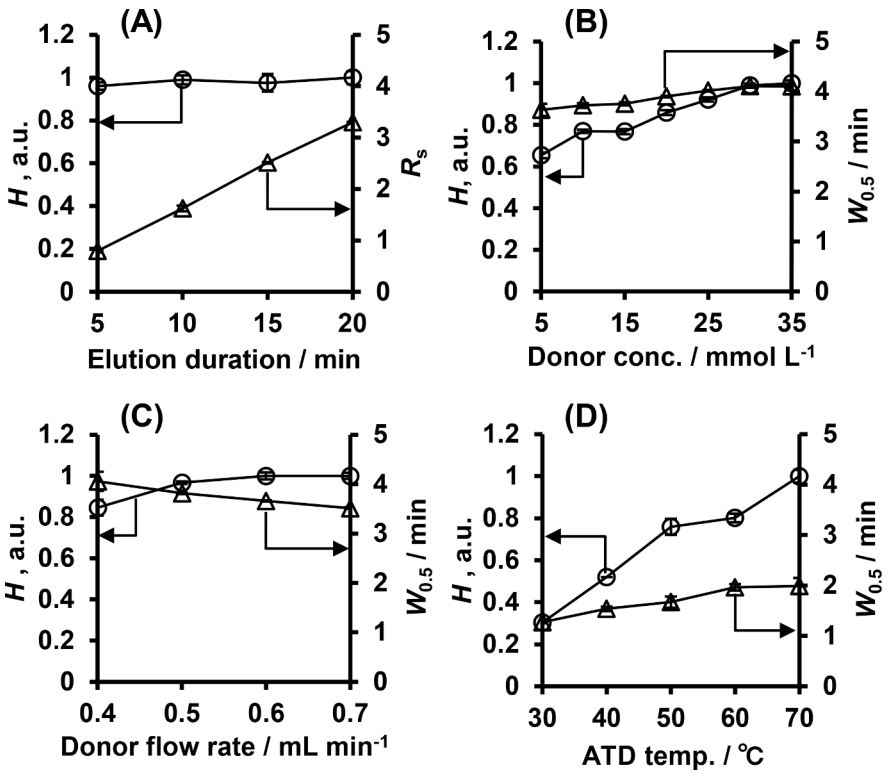

Fig. 2. Optimization of the NH_4^+ detection system, $n \geq 2$. (A) Elution duration from the cation concentrator, operated at 125 μL of 1 mmol L^{-1} NH_4^+ sample, 5 mM NaOH donor@0.5 mL min^{-1}, H_2O receptor@0.5 mL min^{-1}, room temperature. (B) Donor (NaOH) concentration, operated at 125 μL of 1 mmol L^{-1} NH_4^+ sample, 10 min elution duration, NaOH donor@0.5 mL min^{-1}, H_2O receptor@0.5 mL min^{-1}, room temperature. (C) Donor (NaOH) flow rate, operated at 125 μL of 1 mmol L^{-1} NH_4^+ sample, 10 min elution duration, 30 mmol L^{-1} donor, H_2O receptor@0.5 mL min^{-1}, room temperature. (D) ATD temperature, operated at 100 μL of 50 μmol L^{-1} NH_4^+ sample, 10 min elution duration, 30 mmol L^{-1} donor@0.6 mL min^{-1}, H_2O receptor@0.6 mL min^{-1}. H, NH_4^+ peak height; R_s, resolution between two NH_4^+ peaks obtained by sequential sample injection, calculated by $R_s = 1.18\,(t_2 - t_1) / (W_{0.5,2} + W_{0.5,1})$ where t_1 and t_2 are the time of two NH_4^+ peaks (peak 1 appears first), and $W_{0.5,1}$ and $W_{0.5,2}$ are the peak width at half-height for peaks 1 and 2; $W_{0.5}$, NH_4^+ peak width at half-height.

chromatography was accomplished on an ICS-1500 ion chromatographic system (10 mmol L^{-1} methanesulfonic acid eluent at 0.35 mL min^{-1}, two IonPac CS12A 2 × 250 mm separation columns at 40 °C, CDRS 600 2 mm suppressor with recycling mode at 11 mA, TCC-LP1 cation concentrator instead of a sample loop, all from Dionex or Thermo Fisher Scientific).

2.2. Ammonium detection system

A CRD 200 2 mm carbonate removal device (Dionex) was used as the ammonia transfer device, ATD, and its schematic is shown in Fig. 1A. The ATD consists of a gas-permeable membrane tube with a silicone coating (0.2 mm i.d., 0.3 mm o.d., 100 cm length) placed inside an outer tube (1.0 mm i.d., 1.6 mm o.d.). The donor and receptor solutions respectively flow outside and inside the silicone coating membrane tube. Fig. 1B depicts the diagram of ATD-CD for NH_4^+ detection. The sample (NH_4^+) is concentrated on a cation concentrator, CC (IonPac TCC-LP1, Dionex). After loading the sample, an injection valve, IV (Cheminert C2, Valco Instruments), is switched to the injection mode. The donor solution (NaOH), pumped by a peristaltic pump, PP (Rabbit, Rainin), elutes the NH_4^+ retained in the CC. The NH_4^+ is converted to NH_3 by the reaction with NaOH in the process of being sent to the ATD located in an oven, O (CTO-6A, Shimadzu). In the ATD, the gaseous NH_3 permeates the silicone coating porous membrane and dissolves in the receptor solution (H_2O) being pumped by the PP. Of the total ammonia (NH_3 + NH_4^+) dissolved in H_2O, the NH_4^+ is detected by a conductivity detector, CD (CDM-1, Dionex).

The detector signals are recorded on a personal computer with a sampling interval of 0.5 s via an AD converter (midi LOGGER GL240, GRAPHTEC) under software control (GL100_240_840-APS, GRAPHTEC).

2.3. Field measurement of gaseous ammonia

Comparative field measurements of gaseous NH_3 among the ATD-CD and ion chromatographic system were conducted during June 2021 at Kuramoto Campus of Tokushima University, located in the western part of Tokushima, Japan (34°04′N, 134°30′E). The ambient air was sampled from the fourth-floor north window of the Education and Research Building of the Faculty of Pharmacy. In this area, vegetables such as sweet potatoes are flourishing. To the south of the sampling point rises Mount Bizan (290 m above sea level), and 8 km to the east lies the Kii Channel (strait).

Fig. 1C shows the schematic diagram of the ambient NH_3 monitor, a lab-made parallel plate wet denuder, PPWD coupled ATD-CD. The air sample was drawn at 5.0 L min^{-1} using an air pump (DP-40V, VACUTRONICS) and a mass flow controller, MFC (8500MC, KOFLOC). A disposable filter unit (9900-05-BK, Parker Hannifin) was placed upstream of the MFC as a water trap, WT. The PPWD quantitatively collects water-soluble gaseous components in the denuder liquid, H_2O, which flows through the inner wall of the PPWD at 0.25 mL min^{-1} $plate^{-1}$ [24–27]. The effluent from one gas collection plate was delivered online to the ATD-CD. The other sample from the PPWD was simultaneously pumped to the ion chromatographic system, IC, to compare with the ATD-CD data. For the field measurement of gaseous NH_3, both the NH_4^+ detection systems were operated with 30 min time resolution (20 min sample loading to the CC, 10 min injection mode of the IV). In this case, the air volume collected in one analysis is 50 L per detection system. Calibrations were performed offline by injecting standard solutions of NH_4^+.

3. Results and discussion

3.1. Optimization of ammonia transfer device-conductivity detector

The elution duration of NH_4^+ from the CC, donor concentration and its flow rate, receptor flow rate, and ATD temperature were optimized by analyzing NH_4^+ standard samples. Unless otherwise stated, 125 μL of 1 mmol L^{-1} NH_4^+ was injected into the ATD-CD operated with 0.5 mL min^{-1} of donor (5 mM NaOH)/receptor (H_2O) flow rates at room temperature.

The time required for the elution of NH_4^+ from the CC was

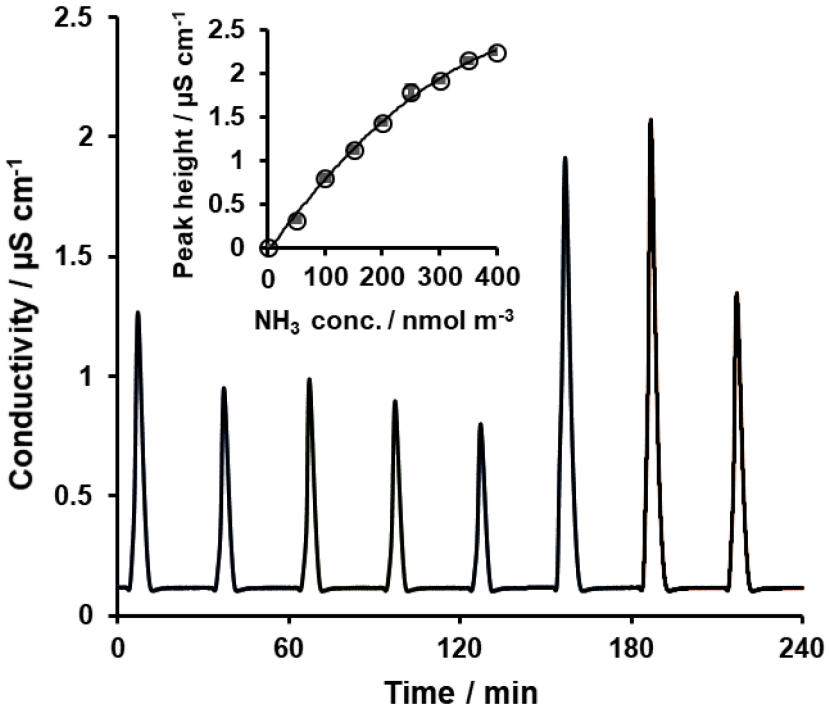

Fig. 3. Typical instrument signal output for a 30 min cycle, sampled from 01:36 to 05:35 on June 5, 2021, in Tokushima, Japan. The inset shows the calibration curve obtained from the NH_3 signal, $n = 2$.

investigated. Acid solutions are generally used to elute cations from cation exchange resins. However, acids such as hydrochloric acid permeate the porous membrane used in the ATD and dissolve in the receptor, potentially interfering with the detection of NH_4^+. The $[NH_3]/[NH_4^+]$ in the eluent increases as the eluent pH increases, and the amount of NH_3 permeating the porous membrane can be expected to increase. Therefore, NaOH solution was tested as the eluent and donor. Fig. 2A shows the NH_4^+ peak height, *H,* and resolution between two NH_4^+ peaks, R_s as a function of elution duration, i.e., the time the NaOH eluent flows through the CC. The *H* remained nearly constant at all elution duration, but the R_s improved with the elution duration increased. We selected 10 min as the time needed for the NH_4^+ elution, as it achieved 1.5 resolution (complete separation, see Fig. S1) in the shortest time.

As shown in Fig. 2B, the *H* and NH_4^+ peak width at half-height, $W_{0.5}$, rose gradually with NaOH donor concentration. The donor pH dominated the $[NH_3]/[NH_4^+]$. At 30 mmol L^{-1} NaOH donor, where the *H* reached a plateau, the theoretical $[NH_3]/[NH_4^+]$ was calculated to be 1687 from the Henderson-Hasselbalch equation with pH = 12.47 and acid dissociation constant of ammonia, $pK_a = 9.25$ [29]. On the other hand, the theoretical value of $[NH_4^+]/[NH_3]$ in the receptor solution (H_2O, pH = 7.00) was calculated to be 179.

The axial dispersion of the sample in the donor/acceptor channels may result in a decline of detection sensitivity due to the broadening of the NH_4^+ peak. Fig. 2C shows the effect of donor flow rate on the *H* and $W_{0.5}$. As the flow rate increased, the $W_{0.5}$ decreased, and the NH_4^+ peak became sharper, while the *H* reached a plateau at 0.6 mL min^{-1}. We chose the donor flow rate of 0.6 mL min^{-1} to account for the reagent consumption. Matching the receptor and donor flow rates allowed us to flow both the donor/receptor solutions with a single peristaltic pump.

Temperature, of course, will play the most vital role in deterring the amount of NH_3 permeating the porous membrane. The rate of NH_3 permeability should be linearly related to the vaporization of NH_3 in the donor, which increases rapidly with temperature. The *H* increased dramatically with increasing the ATD temperature, as shown in Fig. 2D. Although the *H* was expected to grow beyond 70 °C, we decided to set 70 °C as the ATD temperature in consideration of the durability of the module.

3.2. ATD-CD performance

One hundred microliters of 100 µmol L^{-1} NH_4^+ were analyzed with the optimized ATD-CD (10 min elution duration, 30 mmol L^{-1} NaOH donor at 0.6 mL min^{-1}, H_2O receptor at 0.6 mL min^{-1}, 70 °C ATD temperature). The ammonia permeability through the ATD was determined to be 74.0 ± 0.5% ($n = 3$) using ion chromatographic quantitation of NH_4^+. Ammonium was detected as ammonium hydroxide. A quadratic calibration equation must be used for quantitation. The limit of detection, LOD ($S/N = 3$) for NH_4^+ and the repeatability for 100 µmol L^{-1} NH_4^+ were 0.865 µmol L^{-1} (corresponding 86.5 pmol NH_4^+) and 2.75% ($n = 5$), respectively. The LOD of our conductometric NH_4^+ detection system was inferior to the fluorometric FIA based on NH_4^+ and *o*- phthalaldehyde/sulfite reaction: 0.009 µmol L^{-1} (corresponding 1.8 pmol NH_4^+) [15], but meanwhile, comparable to the spectrophotometric flow analysis, e.g., gas diffusion separation/spectrophotometric FIA using Berthelot reagent: 0.278 µmol L^{-1} (corresponding 104.2 pmol NH_4^+) [16], gas permeation/spectrophotometric FIA using Cresol Red indicator: 0.222 µmol L^{-1} (corresponding 66.7 pmol NH_4^+) [17]. The above fluorometric/spectrophotometric systems required reaction reagents for NH_4^+. On the other hand, the only reagent needed in our ATD-CD is NaOH, which was used to convert NH_4^+ to NH_3, and no reagent was required for the conductometric detection of NH_4^+. In addition, our NH_4^+ detection approach is several times more sensitive than a recently reported conductometric method: gas diffusion unit/dual-channel C^4D (capacitively coupled contactless conductance detector) combined FIA (LOD: 1.85 µmol L^{-1}, corresponding 1850 pmol NH_4^+) [21].

3.3. Field measurement

In June 2021, we successfully operated the PPWD coupled optimized ATD-CD for near-real-time monitoring of gaseous NH_3 in Tokushima, Japan. Fig. 3 shows the typical signal output of the ambient air sample. Baseline resolution was achieved in a 30 min analytical window. This

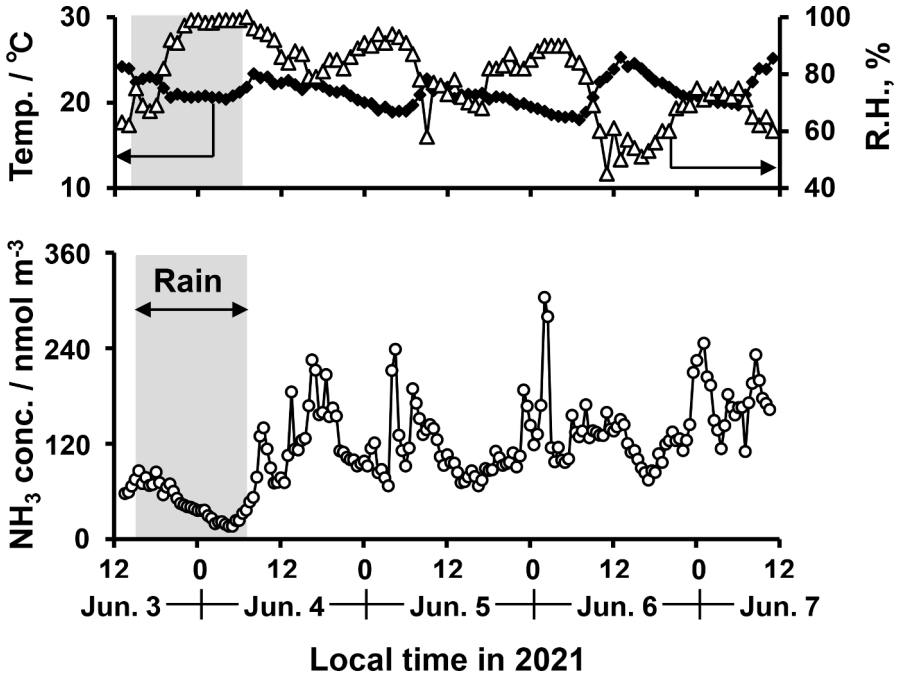

Fig. 4. Temporal variations of atmospheric NH_3 concentration measured by PPWD coupled ATD-CD and meteorological data in Tokushima, Japan.

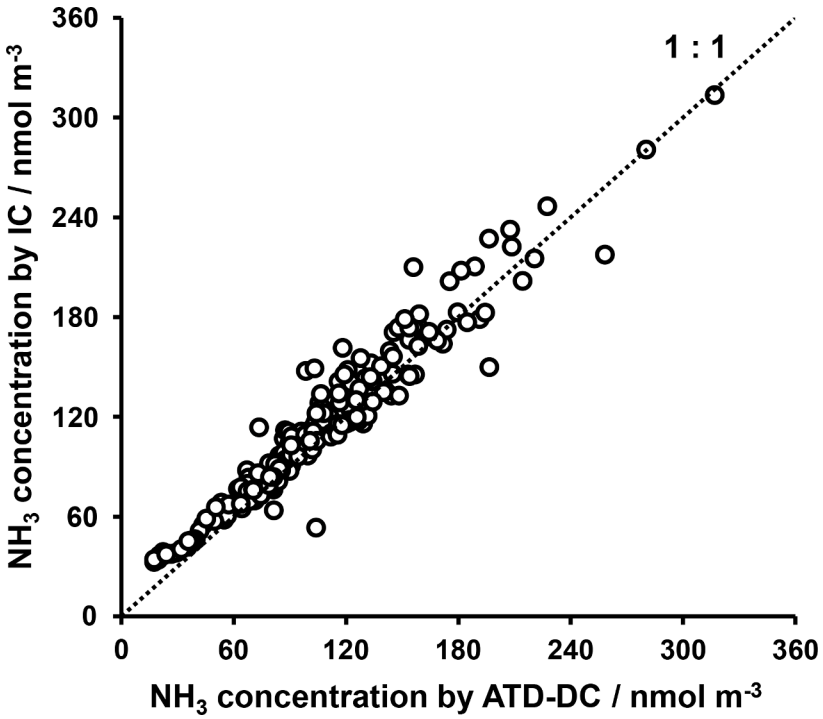

Fig. 5. Scatter plot of the atmospheric NH_3 concentrations detected by ion chromatographic system, IC and ATD-CD in Tokushima, Japan. $n = 186$. The line shown is the 1:1 correspondence line, not the best-fit line.

half-hourly observation allowed us to track a diurnal variation of NH_3 in the atmosphere. The inset and Fig. S2 show, respectively, the calibration curve and signal output in the NH_3 range of 0–400 nmol m^{-3} for a 50 L air sampling. The peak height of the conductivity signal (μS cm^{-1}), *H,* can be expressed as follows.

$$H = - - 0.00000844C^2 + 0.00917C - -0.0502 \quad (1)$$

where C is the gaseous NH_3 concentration (nmol m^{-3}). The determination coefficient of the quadratic calibration equation was satisfactory ($r^2 = 0.997$), and the limit of quantification, LOQ ($S/N = 10$), was calculated to be 11.4 nmol m^{-3}.

Fig. 4 shows the temporal variations of atmospheric NH_3 concentration, temperature, and relative humidity in Tokushima over 5 days. All ambient samples over the observation period ($n = 186$) contained NH_3 above the LOQ. The averaged NH_3 concentration varied widely from 16.5 to 303.8 nmol m^{-3} with an average of 113.0 ± 52.8 nmol m^{-3} and a median of 109.4 nmol m^{-3}. The NH_3 concentration continued to

decrease during the rain period (noon on June 3 – early morning on June 4). Since gaseous NH_3 has high water solubility [26], it is easily scavenged by rainwater and removed from the atmosphere. After the rain stopped, high NH_3 spikes were observed every night between 1 and 3 AM. During this time of day, low temperature and high relative humidity limited the formation of NH_3 by its vaporization from semivolatile ammonium salts such as NH_4NO_3. Wind velocity and direction are vital factors to determine the level of air pollutants. The Kii Channel's strait lies 8 km east of the sampling point. During the night, when the high NH_3 spikes were observed, the land breezes (northwest wind) were blowing from the direction of the significant NH_3 sources, fertile farmlands.

The ambient NH_3 collected by PPWD was measured simultaneously by ion chromatographic system, IC with 30 min time resolution (n = 186). The average and median concentrations of gaseous NH_3 were 116.0 ± 45.3 nmol m^{-3} and 114.5 nmol m^{-3}, respectively. This averaged concentration agreed well with the data detected by ATD-CD, the concentration ratio (IC/ATD-CD) being 1.03 ± 0.62. Fig. 5 depicts the comparison of gaseous NH_3 concentration measured by IC with the data from ATD-CD. The data show excellent agreement, and the best-fit line can be calculated as follows.

$$C_{IC} = (0.953 \pm 0.019)C_{ATD-CD} + (6.26 \pm 1.15) \quad (2)$$

where C_{IC} and $C_{ATD\text{-}CD}$ are the NH_3 concentrations detected by IC and ATD-CD with 30 min time resolution, respectively. We consider that the best-fit slope of 0.953 and the correlation coefficient of 0.964 are excellent. A small number of amines in the atmosphere would permeate the silicone coating porous membrane of ATD. However, the interference seems limited because of the excellent agreement between the ATD-DC and IC results.

In summary, we have demonstrated a simple gaseous NH_3 monitor, PPWD coupled ATD-CD, which allows continuous monitoring of atmospheric NH_3 with 30 min time resolution.

Declaration of Competing Interest

The authors declare that they have no known competing financial interests or personal relationships that could have appeared to influence the work reported in this paper.

Acknowledgments

This research was supported by JSPS KAKENHI Grant Nos. 26340006, 17K00521, and 17KK0011.

Supplementary materials

Supplementary material associated with this article can be found, in the online version, at doi:10.1016/j.talo.2022.100091.

References

[1] J.H. Seinfeld, S.N. Pandis, Atmospheric Chemistry and Physics: from Air Pollution to Climate Change, 1st ed., Wiley-Interscience, New York, 1998.
[2] D.G. Streets, T.C. Bond, G.R. Carmichael, S.D. Fernandes, Q. Fu, D. He, Z. Klimont, S.M. Nelson, N.Y. Tsai, M.Q. Wang, J.H. Woo, K.F. Yarber, An inventory of gaseous and primary aerosol emissions in Asia in the year 2000, J. Geophys. Res. 108 (2003) 8809, https://doi.org/10.1029/2002JD003093.
[3] J.T. Walker, D.R. Whitall, W. Robargec, H.W. Paerl, Ambient ammonia and ammonium aerosol across a region of variable ammonia emission density, Atmos. Environ. 38 (2004) 1235–1246, https://doi.org/10.1016/j.atmosenv.2003.11.027.
[4] C. Reche, M. Viana, M. Pandolfi, A. Alastuey, T. Moreno, F. Amato, A. Ripoll, X. Querol, Urban NH_3 levels and sources in a Mediterranean environment, Atmos. Environ. 57 (2012) 153–164, https://doi.org/10.1016/j.atmosenv.2012.04.021.
[5] C. Perrino, M. Catrambone, A. Di Menno Di Bucchianico, I. Allegrini, Gaseous ammonia in the urban area of Rome, Italy and its relationship with traffic emissions, Atmos. Environ. 36 (2002) 5385–5394, https://doi.org/10.1016/S1352-2310(02)00469-7.
[6] B.J. Finlayson-Pitts, J.N. Pitts, Chemistry of the Upper and Lower Atmosphere: Theory, Experiments, and Applications, 1st ed., Academic Press, San Diego, 1999.
[7] D.Y.H. Pui, S.C. Chen, Z. Zuo, $PM_{2.5}$ in China: measurements, sources, visibility and health effects, and mitigation, Particuology 13 (2014) 1–26, https://doi.org/10.1016/j.partic.2013.11.001.
[8] X. Liu, L. Duan, J. Mo, E. Du, J. Shen, X. Lu, Y. Zhang, X. Zhou, C. He, F. Zhang, Nitrogen deposition and its ecological impact in China: an overview, Environ. Pollut. 159 (2011) 2251–2264, https://doi.org/10.1016/j.envpol.2010.08.002.
[9] D.E. Newby, P.M. Mannucci, G.S. Tell, A.A. Baccarelli, R.D. Brook, K. Donaldson, F. Forastiere, M. Franchini, O.H. Franco, I. Graham, G. Hoek, B. Hoffmann, M. F. Hoylaerts, N. Künzli, N. Mills, J. Pekkanen, A. Peters, M.F. Piepoli, S. Rajagopalan, R.F. Storey, Expert position paper on air pollution and cardiovascular disease, Eur. Heart J. 36 (2015) 83–93, https://doi.org/10.1093/eurheartj/ehu458.
[10] C.A. Pope, A.J. Cohen, R.T. Burnett, Cardiovascular disease and fine particulate matter: lessons and limitations of an integrated exposure response approach, Circ. Res. 122 (2018) 1645–1647, https://doi.org/10.1161/CIRCRESAHA.118.312956.
[11] S.N. Behera, M. Sharma, V.P. Aneja, R. Balasubramanian, Ammonia in the atmosphere: a review on emission sources, atmospheric chemistry and deposition on terrestrial bodies, Environ. Sci. Pollut. Res. 20 (2013) 8092–8131, https://doi.org/10.1007/s11356-013-2051-9.
[12] R.T. Xu, S.F. Pan, J. Chen, G.S. Chen, J. Yang, S.R.S. Dangal, J.P. Shepard, H. Q. Tian, Half-century ammonia emissions from agricultural systems in southern Asia: magnitude, spatiotemporal patterns, and implications for human health, GeoHealth 2 (2018) 40–53, https://doi.org/10.1002/2017GH000098.
[13] H. Volten, J.B. Bergwerff, M. Haaima, D.E. Lolkema, A.J.C. Berkhout, G.R. Hoff, C. J.M. Potma, R.J. Wichink Kruit, W.A.J. van Pul, D.P.J. Swart, Two instruments based on differential optical absorption spectroscopy (DOAS) to measure accurate ammonia concentrations in the atmosphere, Atmos. Meas. Tech. 5 (2012) 412–427, https://doi.org/10.5194/amt-5-413-2012.
[14] D.J. Miller, K. Sun, L. Tao, M.A. Khan, M.A. Zondlo, Open-path, quantum cascade laser-based sensor for high resolution atmospheric ammonia measurements, Atmos. Meas. Tech. Discuss. 6 (2013) 7005–7039, https://doi.org/10.5194/amtd-6-7005-2013.
[15] K. Osada, S. Ueda, T. Egashira, A. Takami, N. Kaneyasu, Measurements of gaseous NH_3 and particulate NH_4^+ in the atmosphere by fluorescent detection after continuous air–water droplet sampling, Aerosol Air Qual. Res. 11 (2011) 170–178, https://doi.org/10.4209/aaqr.2010.11.0101.
[16] T. Yamane, M. Saito, Flow-injection analysis system for simple and rapid determination of ammonia-nitrogen at sub-ppm levels in seawater and concentrated sodium chloride solution, Bull. Soc. Sea Water Sci. Jpn. 49 (1995) 318–320, https://doi.org/10.11457/swsj1965.49.318.
[17] T. Tsuboi, Y. Hirano, Y. Shibata, S. Motomizu, Sensitive determination of ammonia in exhaust gas of thermal power plant using gas permeation/flow injection system, Bunseki Kagaku 51 (2002) 47–51, https://doi.org/10.2116/bunsekikagaku.51.47.
[18] K. Higuchi, A. Inoue, T. Tsuboi, S. Motomizu, Development of a new gas-permeation system and its application to the spectrophotometric determination of ammonium ion by FIA, Bunseki Kagaku 48 (1999) 253–259, https://doi.org/10.2116/bunsekikagaku.48.253.
[19] T. Li, M. Zhou, Z. Fan, X. Li, J. Huang, Y. Wu, H. Zhao, S. Zhang, Online conductimetric flow-through analyzer based on membrane diffusion for ammonia control in wastewater treatment process, ACS Sens. 4 (2019) 1881–1888, https://doi.org/10.1021/acssensors.9b00768.
[20] J. Huang, C.W.K. Chow, P. Kuntke, L. Cruveiller, G. Gnos, D.E. Davey, P. T. Teasdale, The development and evaluation of a microstill with conductance detection for low level ammonia monitoring in chloraminated water, Talanta 200 (2019) 256–262, https://doi.org/10.1016/j.talanta.2019.03.043.
[21] S. Chaneam, P. Inpota, S. Saisarai, P. Wilairat, N. Ratanawimarnwong, K. Uraisin, W. Meesiri, D. Nacapricha, Green analytical method for simultaneous determination of salinity, carbonate and ammoniacal nitrogen in waters using flow injection coupled dual-channel C4D, Talanta 189 (2018) 196–204, https://doi.org/10.1016/j.talanta.2018.06.082.
[22] K. Lin, Y. Zhu, Y. Zhang, H. Lin, Determination of ammonia nitrogen in natural waters: recent advances and applications, Trends Environ. Anal. Chem. 24 (2019) e00073, https://doi.org/10.1016/j.teac.2019.e00073.
[23] M. Zhang, X. Dong, X. Li, Y. Jiang, Y. Li, Y. Liang, Review of separation methods for the determination of ammonium/ammonia in natural water, Trends Environ. Anal. Chem. 24 (2020) e00098, https://doi.org/10.1016/j.teac.2020.e00098.
[24] C.B. Boring, R. Al-Horr, Z. Genfa, P.K. Dasgupta, M.W. Martin, W.F. Smith, Field measurement of acid gases and soluble anions in atmospheric particulate matter using a parallel plate wet denuder and an alternating filter-based automated analysis system, Anal. Chem. 74 (2002) 1256–1268, https://doi.org/10.1021/ac015643r.
[25] M. Takeuchi, H. Tsunoda, H. Tanaka, Y. Shiramizu, Parallel-plate wet denuder coupled ion chromatograph for near-real-time detection of trace acidic gases in clean room air, Anal. Sci. 27 (2011) 805–810, https://doi.org/10.2116/analsci.27.805.
[26] M. Takeuchi, Y. Miyazaki, H. Tsunoda, H. Tanaka, Atmospheric acid gases in Tokushima, Japan, monitored with parallel plate wet denuder coupled ion chromatograph, Anal. Sci. 29 (2013) 165–168, https://doi.org/10.2116/analsci.29.165.
[27] M. Takeuchi, M. Namikawa, K. Okamoto, T. Oda, H. Tanaka, H. Okochi, K. Toda, K. Miura, H. Tanaka, Online analysis of water-soluble acidic gases and anions in

particles at the southeastern foot of Mt. Fuji, Bunseki Kagaku 70 (2021) 65–69, https://doi.org/10.2116/bunsekikagaku.70.65.
[28] S.M.R Ullah, R.L. Adams, K. Srinivasan, P.K. Dasgupta, Asymmetric membrane fiber-based carbon dioxide removal devices for ion chromatography, Anal. Chem. 76 (2004) 7084–7093, https://doi.org/10.1021/ac0492160.
[29] D.R. Lide, CRC Handbook of Chemistry and Physics, 84th ed., CRC Press, Boca Raton, 2003.